Synthesis and Cationic Photopolymerization of Fluorine-Containing Vinyl Ether Monomers for the Hydrophobic Films

Wei Li, Ping Feng, Yingquan Zou, Bo Hai

Department of Applied Chemistry, College of Chemistry, Beijing Normal University, Beijing 100875, China
Correspondence to: Y. Q. Zou (E-mail: zouyq@263.net)

ABSTRACT: Fluorine-containing vinyl ether monomer is a combination of UV-curing technology and low surface energy materials. In this article, a type of fluorine-containing vinyl ether monomer was synthesized by the reaction of fluorinated alcohols, hexafluoroben-zene, 2-vinyloxy ethanol, and sodium hydride. These monomers exhibit low viscosity and good fluidity. The effect of the fluorine content of the monomers on their UV-curing behavior was monitored by photo-differential scanning calorimetry. The photo-polymerization process was efficient because the double-bond conversed sufficiently (>85%) and the curing rate was fast (<20 s). In addition, the surface energy of homopolymer and copolymer films was researched. The surface free energy was very low and could even reach 0.92 mJ m^{-2}. The low surface energy was due to high fluorine content and the diffusion of uncured monomers, which was on the basis of X-ray photoelectron spectroscopy data and observed conversions. The structure of homopolymers and copolymers was one of the most important influences on the surface free energy and the thermal properties. The copolymers exhibited better thermal stability than the homopolymers. All of these results demonstrated that these monomers are suitable for a wide range of practical applications such as UV coatings, UV inks, and photoresists. © 2014 Wiley Periodicals, Inc. J. Appl. Polym. Sci. **2014**, *131*, 41019.

INTRODUCTION

Low surface energy films have experienced rapid development in many high-tech and electronic applications such as coatings on microelectronics that must exhibit excellent water and oil repellent, anti-fingerprint, and anti-scratch properties.[1] Low surface energy film material contains inorganic nanoparticles, organic silicones, and organic fluorocarbons.[2] The inorganic nanoparticles are not stable over a long time. Therefore, the instability and high cost of inorganic nanoparticles prevent their practical use.[3] Organic silicones are commonly used due to their excellent high temperature performance, but a high silicon content is required to achieve low surface energy. In addition, organic silicone films possess a weak anti-scratch property.[4,5] Many organic fluorocarbons have been studied due to their satisfactory properties such as water repellence, chemical resistance, thermal stability, anti-fingerprint, and anti-scratch, that allow for their application in fluorocarbon coatings.[6–8] Currently, research on the UV-cured fluorinated monomers is in its infancy, and its development has been driven by academic interest and their potential practical value.

Various properties of a material depend on its surface structure and the chemical composition of the outermost surface layer.[9,10] The incorporation of fluorine chains into UV-curable

monomers provides an overall improvement in the hydrophobicity of UV-cured polymers, because the fluorine atoms, which exhibit strong polarity, transfer to the surface. Meskini et al. reported super hydrophobic and highly oleophobic films that were obtained from the copolymerization of perfluorinated vinyl ether with vinylidene cyanide.[11] Bongiovanni et al. reported the synthesis of fluorinated monomers and their copolymers with fluorine-free vinyl ether monomers. A low surface energy film was obtained by adding only 3.0 wt % of a fluorine-containing monomer, and the water contact angle of this film was 107°.[12] The presence of fluorine imparts special characteristics to the networks, such as hydrophobicity, oleophobicity, and low surface energy.[13]

Previous studies have primarily focused on free-radical photopolymerization of fluorine-containing acrylate (or methacrylate) monomers.[14–16] These monomers are relatively economical and easily transformed to achieve different properties. However, there are some obvious problems and shortcomings associated with acrylate (or methacrylate) monomers. First, UV-curing is inhibited by oxygen and needs to be carried out under an inert atmosphere, which is operationally inconvenient. Second, all of the monomeric materials have an unpleasant odor and present potential health hazards. In addition, the materials lead to
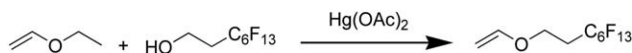
Scheme 1. The synthesis of 1H,1H,2H,2H-perfluorooctyl vinyl ether.

Figure 1. Structures of PAG201.

shrinkage in the reaction volume. In comparison to free-radical systems, epoxides and vinyl ethers are cured via a cationic mechanism that is not inhibited by oxygen, exhibits a low shrinkage during curing and has negligible toxicity.[17–20]

Among UV curing cationic systems, the epoxy system is broadly applied in industrial production.[21,22] However, the vinyl ether system would be a novel alternative system due to the low viscosity, small volume shrinkage, and high curing rate of monomers. 1H,1H,2H,2H-perfluorooctyl vinyl ether and 1H,1H,2H,2H-perfluorodecyl vinyl ether (shown in Scheme 1) have been studied the most.[11,12,23–25] These monomers are prepared by the reaction between fluorinated alcohols with ethyl vinyl ether. However, the reaction condition is harsh and the catalyst is highly toxic. Therefore, only a few fluorinated vinyl ether monomers have been reported, and the high cost makes their applications extremely limited.

Our research group has made several improvements and innovations in the synthesis routes of vinyl ether monomers over the past several years. We have developed a series of low surface energy monomers, such as silicon-containing vinyl ether monomers and fluorine-containing vinyl ether monomers.[4,26,27] The most feasible method for synthesizing fluorine-containing vinyl ether monomers is by the reaction of alcohol and hexafluorobenzene.[28] The reaction conditions are mild, use a nontoxic catalyst, and produce a high yield. In our previous work, we synthesized fluorine-containing vinyl ether monomers using this reaction. When the light intensity is very low (478 μW/cm^2), these monomers still exhibited a rapid curing rate with a high conversion during the photo-polymerization process.[27] Their chemical structures have been characterized. However, systematic studies of their other properties, such as the impact of the fluorine content on the UV-curing behavior, the surface properties of cured films and the thermal properties of polymers, have not been investigated.

Based on our previous work, three fluorinated vinyl ethers with different fluorinated chain length ($C_nF_{2n+1}, n \leq 6$) were synthesized under mild reaction conditions with a nontoxic catalyst and high yield. The viscosity and the UV-curing kinetics of monomers containing different fluorine contents were compared. Fluorinated vinyl ether monomers with vinyl ether carbamate monomers were copolymerized to study the surface properties of these hydrophobic films. Finally, the thermal decomposition mechanism of the homopolymers and copolymers was compared and analyzed.

EXPERIMENTAL

Materials

Hexafluorobenzene, sodium hydride, ethyl vinyl ether, and 1H,1H,2H,2H-perfluorooctane-1-ol were supplied by Alfa Aesar China Ltd (Tianjin, China). The above reagents were used without further purification. Tetrahydrofuran (THF), petroleum ether, and dimethylformamide (DMF) were purchased from the
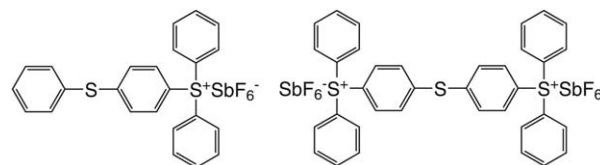
Beijing Chemical Reagent Company (Beijing, China). These organic solvents were distilled, and DMF and THF were dried over calcium hydride and sodium, respectively. The photo-initiator PAG 201 supplied by Power Electronic New Material Co., (Changzhou, China) was a mixture of triphenylhexafluoro-antimonic acid (SbF$_6$) sulfoniumonium salts (Figure 1). The fluorine-containing vinyl ether monomers F1, F2 and fluorine-free vinyl ether carbamate monomers PU1, PU2 (shown in Figure 2) were synthesized according to protocols previously published by our group.[27]

Synthesis of Fluorine-Containing Vinyl Ether Monomer F3

Fluorine-containing vinyl ether monomer F3 was synthesized according to the process shown in Scheme 2.

Sodium hydride (0.72 g, 0.03 mol), 2-(vinyloxy) ethanol (2.64 g, 0.03 mol), and DMF (50 mL) were added to a 250 mL three-necked round-bottomed flask A and the reactants were stirred for 40 min. Then, the reaction mixture was added dropwise to a 500 mL three-necked round-bottomed flask B containing hexafluorobenzene (5.58 g, 0.03 mol) that was previously dissolved in ice-cooled DMF (100 mL). The reaction in flask B was stirred at room temperature for 24 h. After that, sodium hydride (0.72 g, 0.03 mol), 1H,1H,2H,2H-perfluorooctane-1-ol (10.92 g, 0.03 mol), and DMF (50 mL) were placed in another 250 mL three-necked round-bottomed flask C and the mixture was stirred for 40 min. The resulting mixture in flask C was, then, added to flask B and this reaction mixture was stirred at room temperature for 16 h. Finally, the reaction solution in flask B was poured into water to remove the DMF, and the product was extracted using petroleum ether (3 × 50 mL). The extracted liquid was washed with water (3 × 30 mL) and dried with anhydrous MgSO$_4$. The solvent was removed by rotary evaporation and the residue was further purified under reduced pressure (60°C, 10.0 mmHg) to yield the product.

The reactant NaH can react with alcohol to obtain sodium alkoxide. The sodium alkoxide reacts with hexafluorobenzene to get the products and NaF. The feed ratio of NaH, hexafluorobenzene, 2-(vinyloxy) ethanol, 1H,1H,2H,2H-perfluoroocane-1-ol is 2 : 1 : 1 : 1.

The yield of these monomers was higher than 80%. In our previous work, we reported the parameter regarding ^{1}H-NMR spectra, ^{19}F-NMR spectra (Avame PRX500 Bruker-HNMR spectrometer) and IR spectra (Nicolet FT-IR-5700) for monomers F1.[27] In this article, the corresponding chemical structures of monomers F1–F3 were determined by ^{1}H-NMR spectra, ^{13}C NMR spectra, ^{19}F-NMR spectra, and IR spectra.

Monomer F1: Yield: 89%. IR (KBr, cm^{-1}): 1639.6, 1618.1 (—O—C=C), 1202.1 (C—O—C), ^{1}H-NMR (400.0 MHz, CDCl$_3$, δ): 6.41 (dd, J_1 = 6.8 Hz, J_2 = 7.6 Hz, 1H; CH), 4.40 (t, J = 3.6
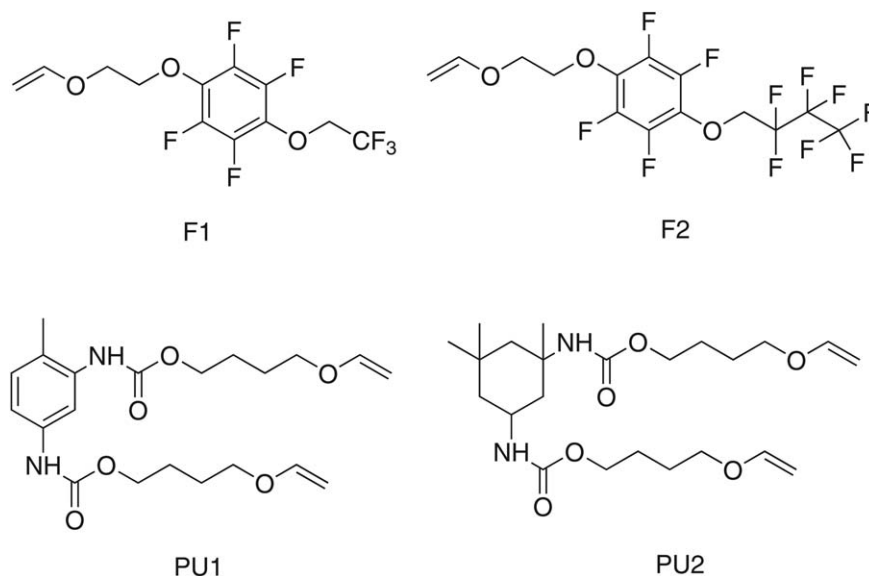
Figure 2. Structures of fluorine-containing vinyl ether monomers F1, F2, and fluorine-free vinyl ether monomers PU1, PU2.

Hz, 2H; CH$_2$), 4.33 (m, 2H; CH$_2$), 4.16 (dd, J_1 = 2.3 Hz, J_2= 12.0 Hz, 1H; CH), 4.00 (dd, J_1 = 2.4 Hz, J_2= 4.4 Hz, 1H; CH), 3.96 (t, 2H, J = 4.6, 2H; CH$_2$). ^{13}C-NMR (100 MHz, CDCl$_3$, δ): 151.19 (s, 1C), 142.94 (m, 1C), 140.30 (m, 2C), 136.83 (m, 2C), 133.48 (m, 1C), 122.57 (dd, 1C-CF$_3$), 87.06 (s, 1C), 73.32(s, 1C), 70.81(m, 1C), 66.69(m, 1C).^{19}F-NMR (400.0 MHz,CDCl$_3$, δ): −74.8 (s, 3F), −156.9 (d, 2F), −167.5 (d, 2F).

*Monomer F2:*Yield: 85%. IR (KBr, cm^{-1}): 1639.6, 1618.1 (—O—C=C), 1202.1 (C—O—C), ^{1}H-NMR (400.0 MHz, CDCl$_3$, δ): 6.41 (dd, J_1 = 6.8 Hz, J_2= 7.6 Hz, 1H; CH), 4.50 (t, J = 12.9 Hz, 2H; CH$_2$), 4.33 (t, J = 13.2 Hz, 2H; CH$_2$), 4.13 (dd, J_1 = 2.3 Hz, J_2= 12.0 Hz, 1H; CH), 4.00 (dd, J_1 = 2.4 Hz, J_2= 4.4 Hz, 1H; CH), 3.94 (m, 4H; CH$_2$). ^{13}C-NMR (100 MHz, CDCl$_3$, δ): 151.20 (s, 1C), 142.80 (m, 1C), 140.44 (m, 2C), 136.75 (m, 2C),
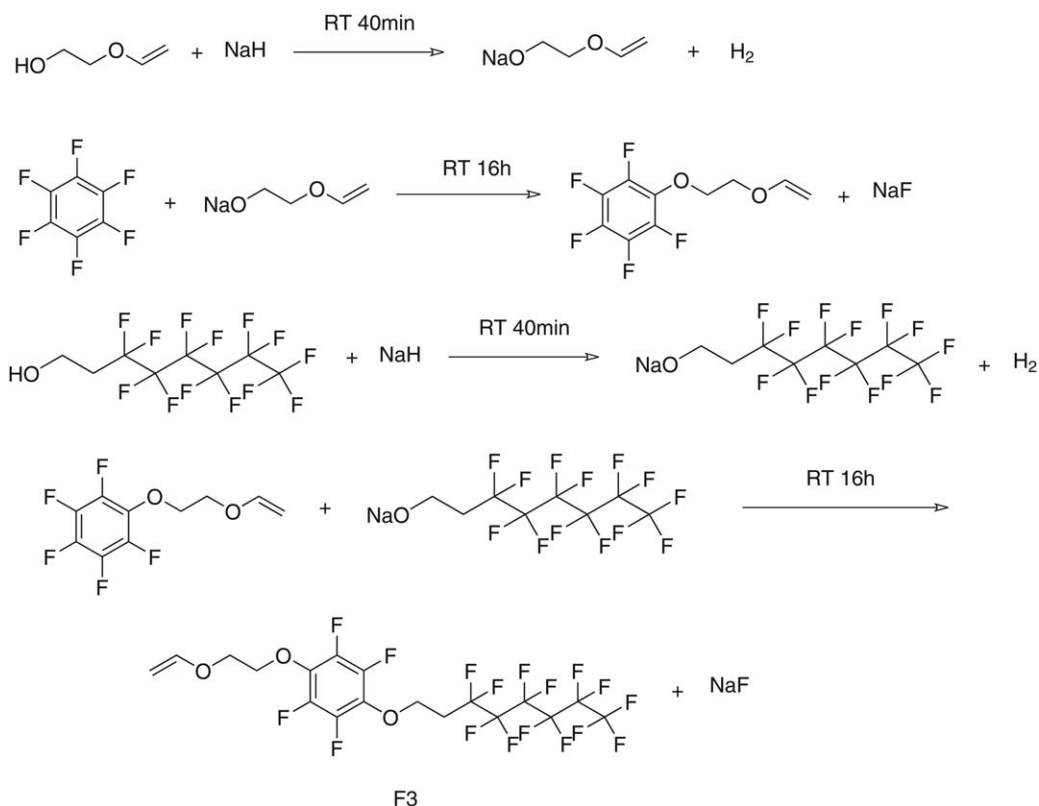
Scheme 2. Synthesis of the UV-curable fluorinated vinyl ether monomer F-3.

Table I. Formulation of the Cationic Systems with Varying Amounts of PU1 or PU2 and F3

Samples	PAG 201 (wt %)	PU1 (mol %)	PU2 (mol %)	F3 (mol %)
F1	3.0	100	–	–
F2	3.0	–	100	–
F3	3.0	–	–	100
PU1-25-F3	3.0	25	–	75
PU1-50-F3	3.0	50	–	50
PU1-75-F3	3.0	75	–	25
PU2-25-F3	3.0	–	25	75
PU2-50-F3	3.0	–	50	50
PU2-75-F3	3.0	–	75	25

133.53 (m, 1C), 119.17 (t, 1C), 116.36 (m, 1C), 114.21 (t, 1C),87.23 (s, 1C), 73.33(s, 1C), 70.23(m, 1C), 66.68(s, 1C).^{19}F-NMR (400.0 MHz,CDCl$_3$, δ): -80.9 (s, 3F), -122.4 (s, 2F), -127.7 (s, 2F),-156.5 (m, 2F), -167.5 (m, 2F).

*Monomer F3:*Yield: 83%. IR (KBr, cm^{-1}): 1639.6, 1618.1 (—O—C=C), 1202.1 (C—O—C), ^{1}H-NMR (400.0 MHz, CDCl$_3$, δ): 6.40 (dd, $J_1 = 6.8$ Hz, $J_2= 7.6$ Hz, 1H; CH), 4.38 (t, $J = 3.6$ Hz, 2H; CH$_2$), 4.32 (t, $J = 4.3$ Hz, 2H; CH$_2$), 4.14 (dd, $J_1 = 2.3$ Hz, $J_2= 12.0$ Hz, 1H; CH), 4.00 (dd, $J_1 = 2.4$ Hz, $J_2= 4.4$ Hz, 1H; CH), 3.92 (t, $J = 13.8$ Hz, 2H; CH$_2$), 2.03 (m, 2H; CH$_2$). ^{13}C-NMR (100 MHz, CDCl$_3$, δ): 151.38 (s, 1C), 141.90 (m, 1C), 140.39 (m, 2C), 136.42 (m, 2C), 133.54 (m, 1C), 120.84 (dd, 1C), 118.34 (dd, 1C), 115.65 (dd, 1C),113.20 (m, 1C), 110.59 (m, 1C),110.59 (m, 1C), 108.23 (m, 1C), 87.04 (s, 1C), 73.30 (s, 1C), 66.65(s, 1C), 54.87(s, 1C), 31.87(s, 1C). ^{19}F-NMR

(400.0 MHz,CDCl$_3$, δ): -80.9 (s, 3F), -113.4 (s, 2F), -122.0 (s, 2F),-123.1 (s, 2F), -123.8 (s, 2F), -126.3 (s, 2F),-156.7 (m, 2F), -163.3 (m, 2F).

(Co) Polymerization and Film Preparation

In this study, we varied the molar percentage of fluorine-free vinyl ether carbamate monomers PU1, PU2and fluorine-containing vinyl ether monomer F3 to investigate the influence of the fluorine content on the surface properties of the films.

The PU1-F3 and PU2-F3 copolymers were prepared in the presence of the photo-initiator PAG 201 (3.0 wt %) with monomer ratios of 25 : 75, 50 : 50, and 75 : 25. PU1–25-F3 indicates that in the formulationPU1 accounts for 25 mol % and F3 accounts for 75 mol %. This nomenclature is also used for the other copolymers. The formulations of the cationic UV-cured systems with varying molar percentages of PU1 or PU2 and F3 monomers are shown in Table I.

UV-curable fluorinated vinyl ether monomer F3 and PU1 were copolymerized according to the process shown in Scheme 3.

Viscosity

The kinematic viscosity of the monomers was evaluated using a capillary viscosity meter (Chinese Glass Instrument Factory, Shenyang, China). The kinematic viscosity of the samples was calculated at 25°C, with units of mm^2/s, using the following formula:

$$v = ct \times (g^0/g') \tag{1}$$

where v is the kinematic viscosity of the samples, c is the coefficient of the viscosity meter, t is the time used by the sample to flow out, g^0 is the standard gravity acceleration speed, and g' is the local gravity acceleration speed.
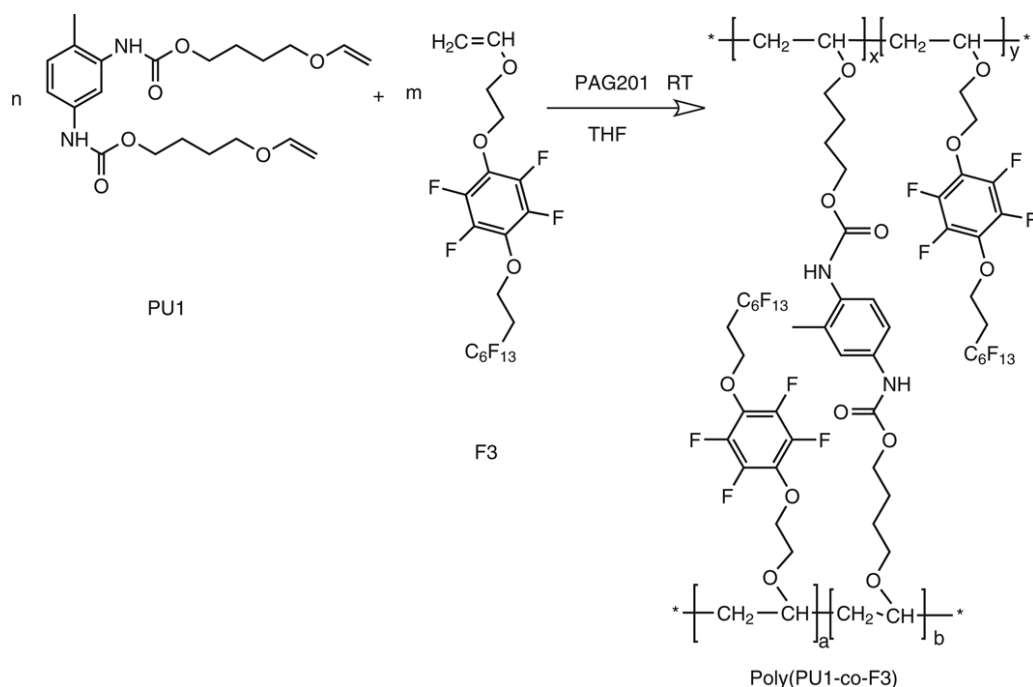
Scheme 3. Cationic copolymerization of PU1 with the fluorinated monomer F3 at room temperature in THF and initiated with PAG 201 (3.0 wt %).

The viscosity of the monomers was obtained by translating the kinematic viscosity to the dynamic viscosity, with units of mPa·s, using the following formula:

$$\eta = \nu \times \rho \qquad (2)$$

where η is the dynamic viscosity of the samples, and ρ is the density of the monomers.

Photo-DSC Experiments
A DSC calorimeter (Q-2000, TA Instruments) equipped with a photocalorimetric accessory was carried out to investigate the kinetics of the UV-cured polymerization. The light source was a 200 W high-pressure mercury lamp that can emit a wavelength range of 200–440 nm. Samples weighing 5.0 ± 0.1 mg were placed in open aluminum pans and the reference aluminum pan was empty when determining the light intensity. The UV light intensity at the sample was 30 mW/cm². The solvent in the sample was evaporated over 30 min prior to UV curing, with the flowing N_2 gas at a rate of 50 mL/min at room temperature.

Static Contact Angle Measurements
The static contact angle measurement was performed at room temperature using a contact angle analyzer (OCA15-EC, Data Physics Instruments, Germany), equipped with a video camera and image analyzer. From the static contact angle, we could determine the hydrophilic property of the UV-curable films. The liquids used for measurement were twice-distilled water and diiodomethane. The temperature and relative humidity were $24 \pm 1.0^\circ$C and $50 \pm 5\%$, respectively. At least five measurements were obtained for each film and the deviation from the average was less than 3°.

X-ray Photoelectron Spectrometer
The surface composition of the UV-cured films was analyzed by an X-ray photoelectron spectrometer (ESCALAB 250Xi, Thermo Scientific Ltd) with an Al Kα X-ray source (1486.6 eV). By measuring the electrons escaping from the film surface at an angle of 90°, we obtained spectra for carbon 1 s (C_{1s}), fluorine 1s (F_{1s}), nitrogen 1s (N_{1s}), and oxygen 1s (O_{1s}). From the peak area, the ratio of the fluorine content on the surface was evaluated. The surface migration ability is reflected by the surface enrichment factor (S_F). S_F is defined as the ratio of the fluorine content at the surface ($F_{surface}$) to the fluorine content in the film (F_{bulk}) as follows:

$$S_F = \frac{F_{surface}}{F_{bulk}} \qquad (3)$$

Thermogravimetric Analysis
The thermal stability of homopolymers and copolymers was monitored by carrying out a thermogravimetric analysis (Mettler-Toledo TGA/DSC 1/1100 instrument). The weight of the samples was 5 mg and the specimens were placed in an aluminum pan and heated at a heating rate of 10°C/min from room temperature to 600°C in air.

RESULTS AND DISCUSSION

The Physical Properties of the Synthetic Monomers
The molecular weight, fluorine content, and viscosity of the three synthesized monomers are shown in Table II. The monomer viscosity is an important indicator for industrial applications. The fluidity of monomers largely depends on their

Table II. The Molecular Weight, Fluorine Content (FC), and the Viscosity of Monomers

Monomers	Molecular weight	FC (wt %)	Viscosity (mPa s, 25°C)
F1	334	39.8	3.61
F2	434	48.3	4.60
F3	598	54.0	5.22

viscosity. When the viscosity of monomers is lower, the monomers exhibit better fluidity.

Based on the data in Table II, the viscosity of the monomers increased as the perfluorocarbon chains extend, which is consistent with a high molecular weight resulting in high viscosity. The fluorine content is a theoretical value obtained by calculating the proportion of fluorine element in the whole molecule. In the general formula, the surface free energy of a polymer can be effectively reduced when the fluorine content of the polymer is more than 20 wt %.[13] The theoretical fluorine content of these three monomers is much greater than 20 wt %.

UV-Curing Kinetics by Photo-DSC
The UV-curing kinetics of the fluorinated vinyl ether monomers and the photo polymerization of the mixtures, which contained fluorinated vinyl ether monomers and fluorine-free vinyl ether monomers were measured by photo-DSC. It is a convenient method for investigating the photo-curing process by analyzing the reaction enthalpy, the kinetic parameter, the degree of conversion, and the curing rate. The measured heat flow can be converted directly to the degree of conversion by the given equation. The figures and tables are obtained by processing the data using the software Origin Pro. 8.5. In addition, photo-polymerization process can be affected by some factors: the intensity of the light source, the species and concentrations of the photo-initiator, the reaction temperature and so forth.

Figure 3 shows the conversion and the curing rate of the UV-curable fluorinated vinyl ether systems. The results of calculation using the following equations are provided in Figure 3(a–d). The conversion of double bonds can be calculated according to the following equation:

$$\alpha = \frac{\Delta H_t}{\Delta H_{total}} \qquad (4)$$

where α is the degree of conversion at time t, ΔH_t is the measured heat enthalpy at time t and ΔH_{total} is the theoretical heat enthalpy for the reaction. The ΔH_{total} value of vinyl ether is 496.9 J/g.[6]

The curing rate (R_p) can be defined as heat flow ($d\alpha/dt$) shown in the following equation:

$$R_p = \frac{d\alpha}{dt} = \frac{dH/dt}{\Delta H_{total}} \qquad (5)$$

where dH/dt is the measured heat flow at a certain temperature.

Figure 3(a) presents the final conversion of each monomer calculated by eq. (4). The final conversion of each monomer occurs in the following order: $F1 > F2 > F3$. The fluorine
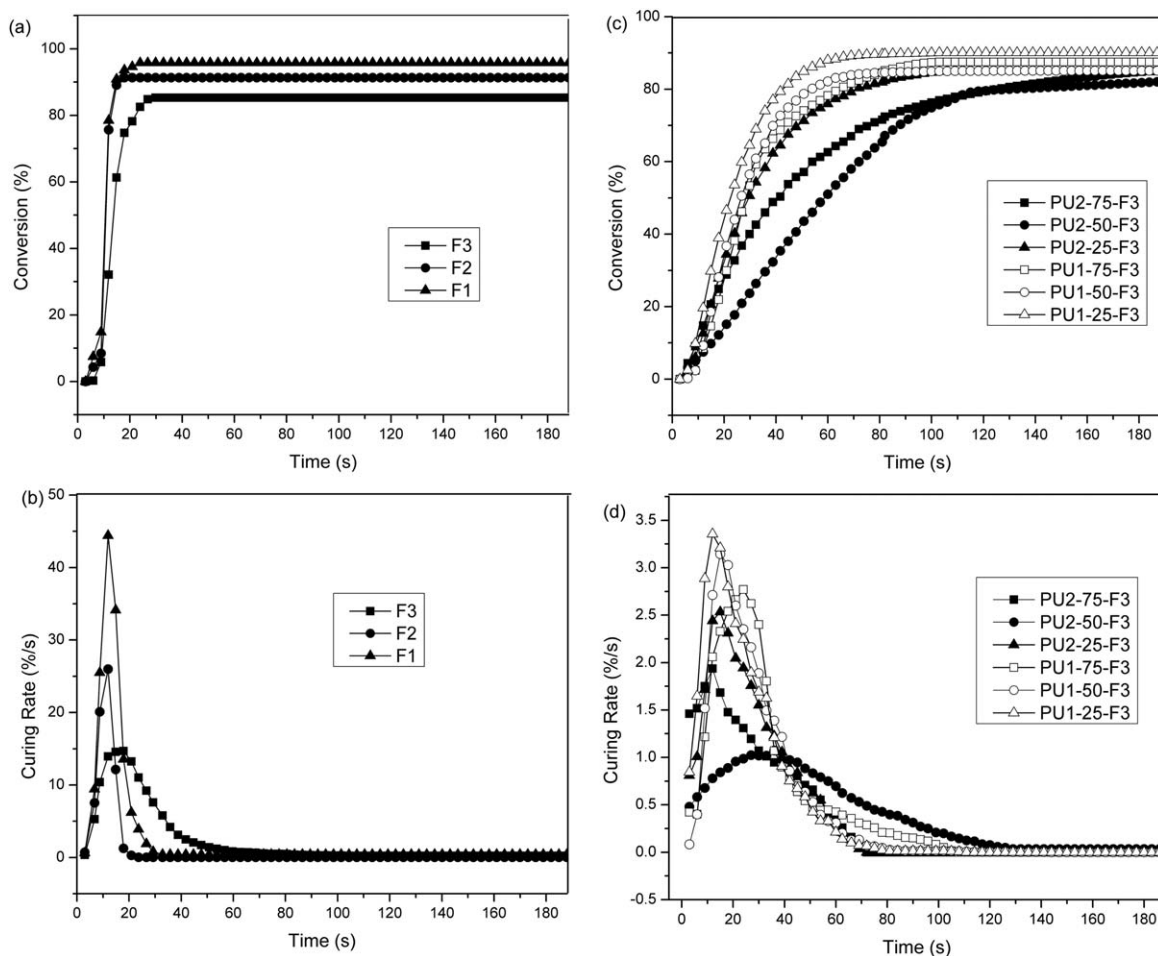
Figure 3. The UV-curing kinetics by photo-DSC. (a) For UV-curable fluorinated vinyl ether monomers: Conversion versus time, (b) For UV-curable fluorinated vinyl ether monomers: curing rate versus time, (c) For copolymers: Conversion versus time, and (d) For copolymers: curing rate versus time. They are photo-cured at 25°C with the following conditions: sample weight = 5.0 mg, sample thickness = ~500 μm, light intensity = 30 mW/cm².

content of monomers has an impact on the UV-curing reaction as shown in Figure 3(a). As the fluorine content increased, the final conversion of these monomers decreased. Figure 3(b) shows that the maximum curing rate of each monomer is in the following order: F1 > F2 > F3. The trend of the conversion is similar to that of the maximum curing rate. The curing rate decreases as the fluorine content increases, which consequently gives rise to a low final conversion. The main reason is that the polarity of fluorine and steric hindrance of the perfluorocarbon chains slow down the reaction.[13]

The parameters in Tables III and IV characterize the curing kinetics of the cationic UV-curing system. The curing rate peak for F1 appears at 11.9 s and the maximum curing rate is 44.4%/s. The peak time and maximum curing rate of F2 are 11.9 s and 26.0%/s, respectively, and for F3, these parameters are 17.9 s and 14.7%/s, respectively. The data indicate that the photo-polymerization process of fluorine-containing monomers is efficient, in which double-bonds converse sufficiently (>85%) and curing rates are fast (<20s).

From the data shown in Figure 3(c,d) and Table IV, the final conversion of these formulations is very similar (82–90%). By

comparing the monomers, the curing rate of the UV-curable formulations containing fluorinated monomers and fluorine-free monomers is quite slow. The maximum curing rate is only 3.4%/s, and the minimum curing rate is 1.0%/s. The UV-curable formulations require more time to complete the photo-polymerization process. As the data shown in Table IV, the final conversion of these formulations is very close and the copolymers may have the similar amount of uncured monomers. Therefore, the free monomer content is not the main influence factor for the surface free energy of the cured films.

Table III. The Reaction Heat Enthalpy, the Peak Time, the Maximum Curing Rate, and the Final Conversion of the UV-Curable Fluorinated Polymers by Photo-DSC

Monomers	ΔH_t (J/g)	Peak time (s)	Maximum curing rate (%/s)	Final conversion (%)
F1	476	11.9	44.4	95.8
F2	454	11.9	26.0	91.3
F3	424	17.9	14.7	85.3

Table IV. The Reaction Heat Enthalpy, the Peak Time, the Maximum Curing Rate, and the Final Conversion of the Mixtures of UV-Curable Fluorinated Monomers and Fluorine-Free Monomers by Photo-DSC

Monomers	ΔH_t (J/g)	Peak time (s)	Maximum curing rate (%/s)	Final conversion (%)
PU1-25-F3	448	11.9	3.4	90.1
PU1-50-F3	424	14.9	3.1	85.3
PU1-75-F3	435	23.9	2.8	87.5
PU2-25-F3	424	14.9	2.5	85.4
PU2-50-F3	407	26.9	1.0	82.0
PU2-75-F3	422	11.9	1.9	84.9

Surface Free Energy

The hydrophilic property of the cured films consists with the high water and CH_2I_2 contact angles which result in a low surface energy. A method based on the Owens–Wendt equation and Young's equation is used for calculating the surface free energy.[29,30]

In the Owens–Wendt equation, the film surface energy (γ) is a sum of dispersion forces (γ^d) and polar forces (γ^p):

$$\gamma = \gamma^d + \gamma^p \tag{6}$$

γ^d and γ^p are solved according to the following eqs (7) and (8), by measuring the water contact angle θ_w and the CH_2I_2 contact angle θ_{dim}:

$$\gamma^d = \frac{1}{\gamma^d_{dim}} \times \left[\frac{\gamma_{dim} \times (\cos\theta_{dim} + 1)}{2} \right] \tag{7}$$

$$\gamma^p = \left[\frac{\gamma_w(\cos\theta_w + 1)}{2} - \frac{\gamma_{dim}(\cos\theta_{dim} + 1)}{2} \right] \times \left[\frac{\gamma^d_w}{\gamma^d_{dim}} \right]^{0.5} \tag{8}$$

The following values for calculating the surface energies are obtained from the literature:[30] $\gamma_w = 72.8$ mJ m^{-2}, $\gamma^d_w = 21.8$ mJ m^{-2}, $\gamma_{dim} = 50.8$ mJ m^{-2}, $\gamma^d_{dim} = 50.8$ mJ m^{-2}.

The contact angles and surface energy parameters of the UV-cured films are shown in Table V and Figure 4.

The contact angle of the UV-cured films increased as the fluorine content increased, which leads to an increase in the film hydrophobicity. The water contact angle and the surface energy of the film Poly-F3 are $138.9 \pm 1.5°$ and 0.92 mJ m^{-2}, respectively, indicating that a hydrophobic surface was obtained. According to the observed conversion, Poly-F3 possesses the highest amount of free monomers that can diffuse and migrate toward the surface decreasing the surface energy.

The fluorine-containing monomers show a sharp decrease in the surface free energy compared to the monomers without fluorine. The surface free energy of PU1 and PU2 is 35.90 and 40.35 mJ m^{-2}, respectively. With the introduction of 25 mol % (13.5 wt %) fluorine-containing monomer F3, the surface free energy of PU1–75-F3 and PU2–75-F3 decrease significantly to 22.38 and 21.90 mJ m^{-2}, respectively. The surface free energy is significantly influenced by only a small amount of fluorine.

For system F1, the water contact angle of 102° is very close to the value typically obtained for fluorinated polymers containing CF$_3$. However, the fluorine content of F1 is much greater than that of PU1-50-F3 and PU2-50-F3, and the surface energy of PU1-50-F3 and PU2-50-F3 is lower than that of F1. Due to the linear structure of poly-F1, the crosslink density is so small that the fluorocarbon chains cannot be arranged closely on the surface. So, the surface energy of poly-F1 cannot decrease effectively. Instead, the cross-linked structures of the copolymers resulting in the C$_6$F$_{13}$ groups form a denser and protective layer with very low surface energy, and the migration ability to the

Table V. Surface Energy Characteristics of the UV-Cured Films

Samples	Fluorine content (wt %)	Contact angle (°)		Surface free energy ^{d}(mJ/m^2)		
		θ_w^a	θ_{dim}^b	γ^{dc}	γ^{pd}	γ^e
F1	39.8	102.8 ± 2.0	60.4 ± 1.7	29.32	−6.15	23.17
F2	48.2	119.7 ± 2.3	100.2 ± 1.9	8.83	−1.71	7.12
F3	54.0	138.9 ± 1.5	104.2 ± 1.5	7.49	−6.57	0.92
PU1-25-F3	40.5	119.1 ± 2.4	87.4 ± 2.1	14.43	−5.29	9.14
PU1-50-F3	27.0	110.2 ± 2.7	79.8 ± 3.2	18.48	−4.18	14.30
PU1-75-F3	13.5	95.9 ± 2.2	70.5 ± 1.6	23.19	−0.81	22.38
PU2-25-F3	40.5	121.7 ± 2.6	88.6 ± 1.7	13.68	−5.81	7.87
PU2-50-F3	27.0	114.2 ± 0.9	97.9 ± 1.3	9.66	−0.18	9.48
PU2-75-F3	13.5	94.3 ± 2.7	75.2 ± 2.8	20.65	1.25	21.90
PU1	0	79.2 ± 0.7	51.5 ± 1.3	34.60	1.30	35.90
PU2	0	74.6 ± 1.5	44.7 ± 2.7	38.52	1.83	40.35
GLASS	–	21.8 ± 1.4	47.4 ± 2.6	36.65	18.32	54.97

^{a} Contact angle by water.
^{b} Contact angle by diiodomethane.
^{c} γ^d = dispersion forces.
^{d} γ^p = polar forces.
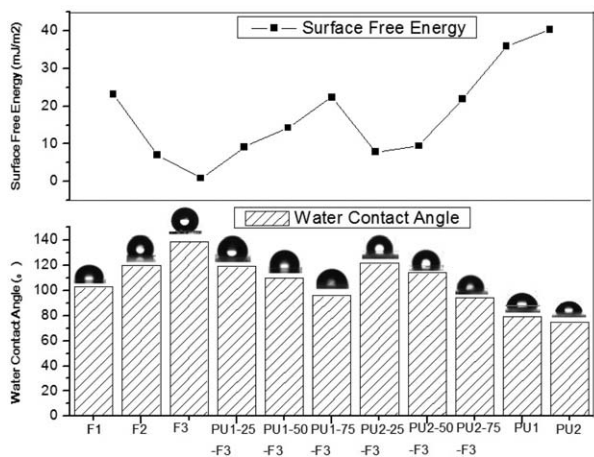^{e} γ = surface energy.

Figure 4. The contact angle and surface energy characteristics of the UV-cured films.

outermost surface of the C_6F_{13} group is better than that of the CF_3 group.

Besides, according the observed conversion, poly-F3 has the most uncured monomers which can migrate to the surface to increase the fluorine content of the surface. So we can obtain the highest water contact angle on poly-F3 films.

XPS Analysis

XPS provides direct information about the relative concentrations of various atoms on the surface. It is crucial method to determine the composition of the external layer (2–3 nm) of the films. On the basis of the atom concentrations, the functional groups can get matched. The XPS spectra of the UV-cured films are shown in Figure 5. The photoemission peaks of the F_{1s}, O_{1s}, C_{1s}, and N_{1s} are observed with bonding energies of 688, 532, 285, and 400 eV, respectively.

The measured fluorine content at the surface ($F_{surface}$), the estimated atomic% fluorine in the film solids (F_{bulk}) and the surface enrichment factor (S_F) are given in Table VI. All of the samples, except F1, exhibit a greater fluorine content at the surface than that estimated in the bulk, indicating that the C_3F_7 and C_6F_{13} groups efficiently migrate to the outermost surface of the films. The data of S_F show that the C_6F_{13} groups migrate easier than the C_3F_7 groups. However, the CF_3 groups do not migrate well. These results suggest that the surface energy is related to the fluorinated monomer concentrations as well as
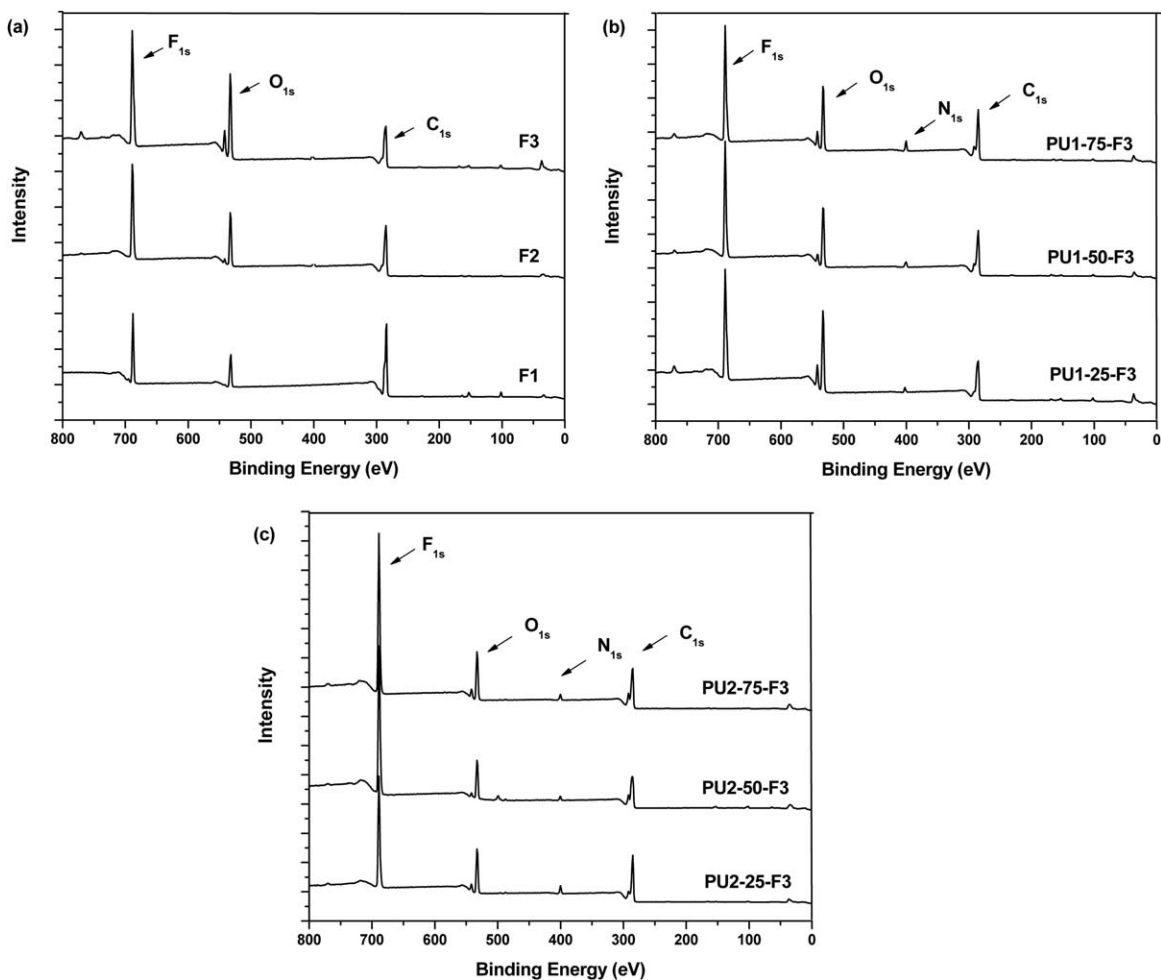

Figure 5. X-ray photoelectron spectroscopy of the UV-cured films: sample thickness = ∼500 μm.

Table VI. Fluorine Content of the Experimental Formulations, XPS Surface Concentrations, and the Surface Enrichment Factor

|	Estimated atomic % fluorine in the UV-cured films (F_{bulk})	Atomic % fluorine at the surface as measured by XPS ($F_{surface}$)	Surface enrichment factor (S_F)
F1	22.580	17.791	0.79
F2	29.729	35.050	1.18
F3	34.694	53.490	1.54
PU1-25-F3	24.402	39.770	1.63
PU1-50-F3	15.596	23.242	1.49
PU1-75-F3	7.489	16.325	2.18
PU2-25-F3	23.394	31.647	1.35
PU2-50-F3	14.407	24.651	1.71
PU2-75-F3	6.693	15.475	2.31

the migration ability of the perfluorocarbon chains to the surface.

The diffusion of free monomers toward the surface is one of the important factors. On the basis of the observed conversion which follows the order: F3 < F2 < F1, the amount of free monomers follows the order: F3 > F2 > F1. Therefore, poly-F3 has the most amount of free monomers which can diffuse and migrate toward the surface to decrease the surface energy. For copolymers, the observed conversion follows the order: PU1-25-F3 (90.1%) > PU1-75-F3 (87.5%) > PU2-25-F3 (85.4%) > PU1-50-F3 (85.3%) > PU1-75-F3 (84.9%) > PU1-50-F3 (82.0%). The conversion of these copolymers is similar and their structures are more cross-linked and complicated. Therefore, the diffusion of free monomers in copolymer can only affect the results but not decide the results.

Thermal Properties of the UV-Cured Films

The thermal stability of the UV-cured films is investigated by TGA analysis. The temperature range of the weight loss curves is from 25 to 600°C. Figure 6(a,b) presents the weight loss curves of homopolymers and copolymers, respectively. According to the thermogravimetric analysis, the poly (PU-*alt*-F3) copolymers exhibit better thermal stability than that of the respective homopolymers.

Several thermal decomposition temperature parameters of homopolymers and copolymers are listed in Table VII, including: the temperature of the initial 10% weight loss (T10%), the temperature of the 50% weight loss (T50%), and the weight loss percent at 460°C. By analyzing these temperature parameters, the three-stage thermal degradation mechanism of the homopolymers can be built. The first stage of the degradation at 116–288°C, involves the decomposition of individual uncured monomers and small molecular weight products. The second stage of degradation at 288–400°C, corresponds to the decomposition of the fluorine-containing side chains and the resulting residue of this stage is a phenolic side chain polymer.[31] The final stage, which occurs at 400–600°C, involves the cleavage of the fluorine-containing phenolic group which is volatile at high temperatures. The linear structure of homopolymers makes
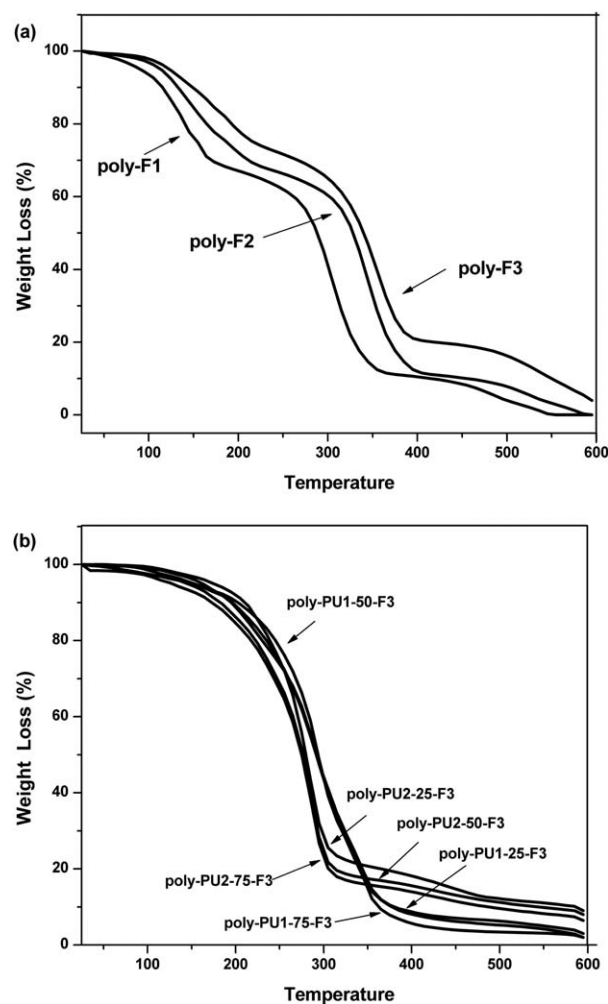
Figure 6. TGA analysis of all the UV-cured films: (a) homopolymers and (b) copolymers.

them not link tightly. In general, homopolymer could not become high molecular weight products which are not volatile.

However, the thermal degradation mechanism of copolymers is only one stage. The reason is perhaps that the cross-linked

Table VII. Characteristic Thermal Decomposition Data for the UV-Cured Films

Samples	Weight loss		
	$T_{10\%}$ (°C)	$T_{50\%}$ (°C)	wt % at 460°C
poly-F1	116.2	287.0	7.59
poly-F2	131.0	328.2	9.87
Poly-F3	145.2	342.3	18.84
poly(F3-PU1-25)	194.8	291.6	6.88
poly(F3-PU1-50)	202.8	293.8	5.99
poly(F3-PU1-75)	191.7	286.2	4.05
poly(F3-PU2-25)	207.2	281.8	13.77
poly(F3-PU2-50)	183.3	276.5	12.62
poly(F3-PU2-75)	174.0	279.8	10.99

structures of copolymers make the uncured monomers wrapped in the inner part of sufficiently cured copolymers. Figure 6(b) and Table VII show the temperature at which the copolymers start to decompose (94°C, 2% weight loss), leading to 50% weight loss around 280°C. However, in Figure 6(b) and Table VII, homopolymers start to decompose at 80°C (2% weight loss), and lead to 50% weight loss around 320°C. From these results, the thermal stability of copolymers performs better than homopolymers.

The first stage of thermal degradation (116–288°C) involving the decomposition of individual uncured monomers and small molecular weight products follows the order F1 > F2 > F3. But the amount of free monomer, from Figure 1, follows the order F3 > F2 > F1. This inconsistency may be influenced by three factors. First, the cationic photo polymerization always exhibits dark-curing behavior. Even if the UV light is removed, the existence of hydrogen protons still can initiate the curing reaction. So, the final conversion of these three monomers might have small difference. Second, in general, the higher the molecular weight of the monomer, the better the thermal stability. The decomposition of free monomers depends mainly on their molecular weights and structures, and not on the amount. Third, the homopolymers have linear structures, and they cannot become the macromolecules which show good thermal stability. Comparing with F2 and F3, monomer F1 only has $-CF_3$ group, and cannot form a dense and protective layer. Therefore, the thermal stability of Poly-F1 is the poorest. In terms of the molecular weight and the structure, this inconsistency can be explained.

CONCLUSIONS

UV-curable vinyl ether monomers with perfluorinated aromatic units were designed and synthesized. The synthetic method uses mild conditions and produces high yields. These monomers exhibited excellent UV-curing behaviors, which is evident from their high double-bond conversion (>85%) and fast curing rate (<20 s). Moreover, the fluorine-containing monomers exhibited low viscosity and remarkable liquidity. UV-cured films exhibited a relatively lower surface energy (less than 1.0 mJ m^{-2}), which could increase their hydrophobic properties. The low surface tension of these films was influenced by the high fluorine content of the surface and the diffusion of uncured monomers to the surface. The results indicated that the poly-F3 had the lowest conversion and the most amount of uncured monomers which can migrate to the surface to increase the fluorine content and decrease the surface free energy. The homopolymers and copolymers exhibited excellent thermal stability. Due to the linear nature of homopolymers and the cross-linked nature of copolymers, the thermal stability of copolymers performs better than homopolymers. In conclusion, fluorine-containing vinyl ether monomers are suitable for use as photosensitive compounds, and have a wide range of practical applications such as in UV coatings, UV inks, and photoresists.

ACKNOWLEDGMENTS

REFERENCES

1. Walter, N.; Tommaso, B.; Dmitrij, C.; Maria, V. D.; Mariapia, P.; Luca, M.; Giuseppe, R. *J. Coat. Technol. Res.* **2011**, *8*, 153.

2. Ma, M.; Hill, R. M. *Curr. Opin. Colloid Interface Sci.* **2006**, *11*, 193.

3. Yin, Y.; Alivisatos, A. P. *Nature* **2005**, *437*, 664.

4. Fang, Y.; Zou, Y. Q. *Polym. Int.* **2013**, *62*, 1624.

5. Wang, S. Y.; Zou, Y. Q. *J. Appl. Polym. Sci.* **2013**, *129*, 3325.

6. Jung, D. C.; Jin, W. H. *J. Appl. Polym. Sci.* **2005**, *97*, 1345.

7. Toyoko, I. *Curr. Opin. Colloid Interface Sci.* **2003**, *8*, 307.

8. Jung, D. C.; Jin, W. H. *Eur. Polym. J.* **2005**, *41*, 367.

9. Sangermano, M.; Bongiovanni, R.; Malucelli, G. *J Appl. Polym. Sci.* **2003**, *89*, 1524.

10. Mary, J. A.; Scott, A. M. *J. Environ. Sci. Technol.* **2006**, *40*, 1447.

11. Meskini, A.; Raihane, M.; Ameduri, B. *Macromolecules* **2009**, *42*, 3532.

12. Bongiovanni, R.; Sangermano, M.; Malucelli, G.; Priola, A.; Leonardi, A.; Ameduri, B.; Pollicino, A.; Recca, A. *J. Polym. Sci. Part A: Polym. Chem.* **2003**, *47*, 2890.

13. Hyeon, D. H.; Hyun, J. K. *J. Colloid Interface Sci.* **2011**, *362*, 274.

14. Vitale, A.; Priola, A.; Tonelli, C.; Bongiovanni, R. *Polym. Int.* **2013**, *62*, 1395.

15. Tuba, C. C.; Ersin, S. *Prog. Org. Coat.* **2013**, *76*, 388.

16. Dreher, W. R.; Jarrett, W. L. *Macromolecules* **2005**, *38*, 2205.

17. Yukari, O.; Tomohiro, T.; Shokyoku, K.; Sadahito, A. *J. Polym. Sci. Part A: Polym. Chem.* **2012**, *50*, 2993.

18. Bongiovanni, R.; Medici, A.; Zompatori, A.; Garavaglia, S.; Tonelli, C. *Polym. Int.* **2011**, *61*, 65.

19. Ito, H.; Houle, F. A. *Proc. SPIE* **2006**, *6153*, 61531A.

20. Golaz, B.; Michaud, V.; Leterrier, Y.; Manson, J. *Polym. J.* **2012**, *53*, 2038.

21. Wang, C.; Zuo, Y. *J. Polym. Sci. Part A: Polym. Chem.* **2009**, *114*, 2528.

22. Brostow, W.; Chonkaew, W.; Menard, K. P. *Mater. Sci. Eng. A* **2009**, *507*, 241.

23. Zeng, Z. H.; Yang, J. W.; Pang, L. X.; Chen, Y. L. *Polym. Int.* **2006**, *55*, 353.

24. Bongiovanni, R.; Malucelli, G.; Sangermano, M.; Priola, A. *J. Fluorine Chem.* **2004**, *125*, 345.

25. Vandooren, C.; Jerome, R.; Teyssie, P. *Polym. Bull.* **1994**, *32*, 387.

26. Xiao, S. Z.; Zou, Y. Q. *Chem. J. Chin. Univ.* **2011**, *32*, 383.

27. Li, W.; Zou, Y. Q. *Proc. SPIE* **2012**, *8325*, 83251V.

28. Song, B.; Park, J. K.; Kim, H. K. *J. Polym. Sci. Part A: Polym. Chem.* **2004**, *42*, 6375.

29. Zheng, J. F.; He, A. H.; Li, J. X.; Xu, J.; Han, C. C. *Polym. J.* **2006**, *47*, 7095.

30. Van ,O. C.; Good, R. J.; Chaundhury, M. K. *Langmuir* **1998**, *4*, 884.

31. Valter, C.; Gianluca, B. P.; Francesco, C. *Macromol. Chem. Phys.* **2001**, *202*, 2093.